

# Force control of grinding based on frequency analysis

Yuya Nogi<sup>1</sup>, Sho Sakaino<sup>2</sup>, Toshiaki Tsuji<sup>1</sup>,

**Abstract**—Hysteresis-induced drift is a major issue in the detection of force induced during grinding and cutting operations. In this paper, we propose an external force estimation method based on the Mel spectrogram of the force obtained from a force sensor. We focus on the frequent strong correlation between the vibration frequency and the external force in operations with periodic vibrations. The frequency information is found to be more effective for an accurate force estimation than the amplitude in cases with large noise caused by vibration. We experimentally demonstrate that the force estimation method that combines the Mel spectrogram with a neural network is robust against drift.

**Index Terms**—force sensing, force control, grinding, frequency analysis

## I. INTRODUCTION

MANY manufacturing processes, such as assembly and grinding, involve contact with objects. The variability in the state of contact with an object often increases with increasing task complexity. The automation of tasks with changing contact states, which are called contact-rich tasks, has been widely studied in robotics [1]–[3]. In contact-rich tasks, the contact force varies considerably with the contact state changes. In such tasks, small fluctuations in the force must be detected to determine whether contact is possible. In addition to the detection of large forces, the extraction of features from low forces requires force measurement with a wide dynamic range [4]; hence, force sensing is an important technology influencing the performance of contact-rich tasks. Force sensing often limits the performance in simple tasks; wherein few changes occur in the contact state. For example, in grinding, the magnitude of the contact force significantly affects the quality of the product surface [5], and it is desirable to control the contact force to a constant or desired magnitude. Force control techniques, such as hybrid control [6] and impedance control [7], are widely used to adjust the force to a desired value in tasks involving contact. Attempts have been made to improve the performance of these methods [8], [9]. The most important factor determining the performance of such control methods is force sensing. However, problems, such as hysteresis, temperature drift, and deviation of the offset values in the working posture, cause steady-state errors in the force information. In addition, there is fluctuation in the obtained force data because of the vibration of the tool

\*This work was partially supported by JSPS KAKENHI, Japan Grant Number 21H01280.

<sup>1</sup>Yuya Nogi and Toshiaki Tsuji are with the Dept. Electrical and Electronic Systems, Saitama University, 255 Shimo-okubo, Saitama, 338-8570

<sup>2</sup>Sho Sakaino is with the Graduate School of Systems and Information Engineering, University of Tsukuba, 1-1-1 Tennodai, Tsukuba, Ibaraki 305-8577

attached to the end-effector (EEF) during grinding and cutting. If such force information is used in the control system without considering these problems, chattering may occur, and force control may become unstable.

Hence, attempts to improve force control using force information with less noise are underway. The external force estimation observer is a technique for estimating the force from the joint torque using an observer instead of acquiring it using a force sensor [10]; however, noise caused by static friction is an issue when a geared motor is used. The force information can be estimated from the joint torque applied to a grinding work [11], and many attempts have been made to estimate the joint torque from series elastic actuator displacement and to use it for force control [12]–[14]. Unfortunately, in methods that infer the force from the joint torque of the robot, the inertial forces of the links connected in series cause noise. Despite the attempts made to improve the accuracy of force sensors [15], the hysteresis of six-axis force sensors may occur up to approximately 1% of the full scale, which limits the detection of fine contact.

In this study, we focus on the frequent strong correlation between the vibration frequency and the external force in operations with periodic vibrations, such as grinding and cutting. The frequency information is found to be more effective than the amplitude for accurate force estimation in noisy tasks. In addition, it is more robust against problems specific to force sensors, such as hysteresis. Although the correlation between the force information and the frequency components is strong, the relationship is highly nonlinear. Therefore, we introduce a neural network (NN)-based machine learning method for inference. Many attempts have been made to improve force estimation and force control using neural networks [16], [17]; however, none have shown that the control performance can be improved by combining them with a real-time frequency analysis. Through practical experiments, we evaluate the accuracy of force estimation and the performance of the grinding operation on a flat surface using a six-degree-of-freedom (6-DOF) manipulator and demonstrate the effectiveness of the proposed method.

The remainder of this paper is organized as follows. Section II describes the principle of the proposed method. Section III presents the experiments and their results, demonstrating the effectiveness of the proposed method. Finally, Section IV summarizes this paper.

## II. METHODS

In this section, we first describe the experimental setup and the verification task, namely grinding, to clarify the precon-

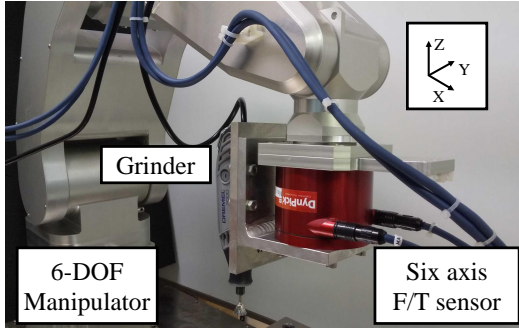


Fig. 1. Experimental setup.

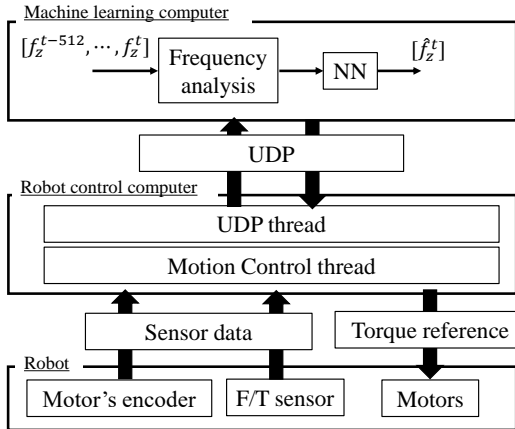


Fig. 2. System architecture.

ditions for this study. Next, the characteristics of the force information and frequency analysis of the grinding process are described. Finally, the machine learning model is discussed.

#### A. Prerequisites

Fig. 1 shows the robot used in this study. A 6-DOF manipulator, equipped with a six-axis force/torque (F/T) sensor and a rotor as a tool for grinding, was used in the experiments. The rotor was not equipped with additional sensors (e.g., speed sensor); thus, the experiment could be performed with a general industrial robot setup. Fig. 2 shows the system configuration of the proposed method. Two PCs for control and force prediction were used. User Datagram Protocol (UDP) communication was used between the control PC and the force prediction PC to send and receive data. The control PC had an Intel Core i7-10700K CPU, and the force prediction PC had an Intel Core i9-10989XE CPU and a GeForce GTX1660 SUPER GPU.

Fig. 3 shows the force response of the force sensor when it was pushed up and down by hand nine times alternately. A steady response remained even during the period when the external force was removed after the push. This steady response is due to the hysteresis of the force sensors, which is the main cause of error in various types of force sensors. In this test, the average value of the hysteresis after applying a force of approximately 100 N was 4.31 N, and its variance

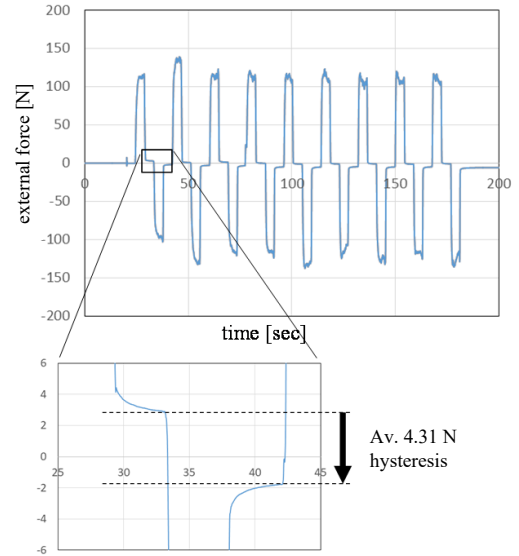


Fig. 3. Force response and hysteresis in the experimental machine used.

was 1.54 N. These results show that grinding with this robot may result in an error of a few Newtons due to hysteresis.

#### B. Concept of this study

Grinding is adopted as a typical task in which the force fluctuates because of the influence of the tool used. Fig. 4 shows the concept of this study. In conventional force control, the information from the force sensor is used as it is or is processed using a nonlinear regression method (e.g., low-pass filter (LPF)) to improve the force estimation accuracy and the performance of the feedback control. In this study, we show that the varying force information can be converted into more accurate force information by adding a frequency analysis to the nonlinear regression process. A NN-based machine-learning method was used as the nonlinear regression model.

For the evaluation, we also adopted the force information obtained from a worktable-type force sensor [18] as the correct answer label. Because this sensor is an installed type, it is unaffected by the drift due to the working posture; in addition, this sensor is recalibrated from the response when the robot is not in contact with it to realize an accurate measurement. Moreover, because the sensor is not directly attached to the tool, it is not susceptible to vibrations. The sampling time of both the EEF and worktable-type force sensors was 1 ms.

#### C. Feature Representation of Mel spectrogram

In this study, we focused on the vibration of the force information. In tasks, such as grinding and cutting, the vibration of the tool also affects the force information. Therefore, it is necessary to extract features from oscillatory signals. Thus, we used the Mel spectrogram (MS) [19], [20] as a real-time frequency analysis. The MS is calculated based on the short-time Fourier transform (STFT) and is obtained by applying a nonlinear transformation to the frequency axis of the STFT, which calculates the frequency information with

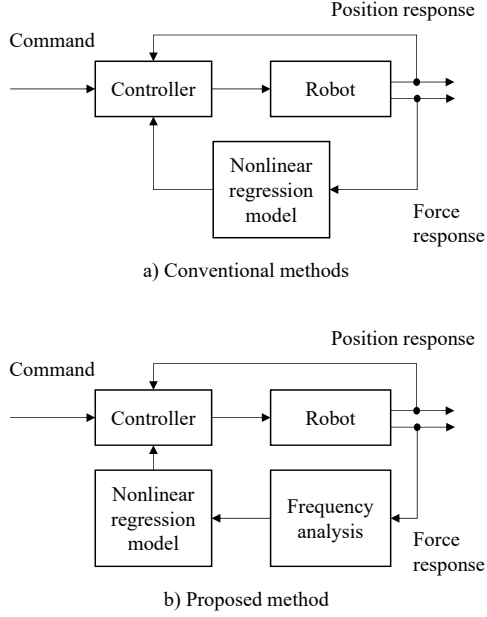


Fig. 4. Concept of this study.

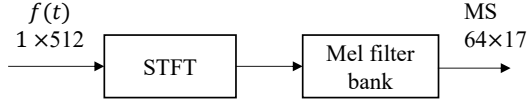


Fig. 5. Conceptual diagram of the process of calculating Mel spectrogram.

a smaller number of dimensions considering human auditory characteristics. By deriving the MS, it is expected that the force information can be represented in a lower dimension. The Mel scale (*mel*) is converted from the frequency (*f*) using the following equation:

$$mel = 2595 \log\left(1 + \frac{f}{700}\right) \quad (1)$$

The number of data points that can be acquired is limited because of the online estimation of the force information. Therefore, in this study, 512 samples (512 ms) were used to calculate the MS. Fig. 5 shows a conceptual diagram of the MS calculation, performed by STFT using a 256 ms frame size, 32 ms frame hop, and Hann window function. A 64-channel Mel filter bank was applied to the calculated STFT.

Typically, a pre-emphasis filter is introduced as a pre-processing step in speech processing [21]. However, in this study, we used raw data from the force sensor because the bandwidth of the force information was shorter than that of the speech.

Fig. 6 shows the features of the force information for each force sensor. The left figure shows the case where the contact force is around 1 N, and the right figure shows the case where the contact force is around 3 N. Fig. 6(a) shows the force information of the EEF force sensor. Fig. 6(b) shows the force information obtained by applying a first-order LPF with a cutoff frequency of 5 Hz to (a) and the force information of the worktable-type force sensor. Fig. 6(c) presents the MS

calculated from the force information in (a). From the results of (b) and (c), it can be confirmed that the MS varies with the contact force. Therefore, the contact force can be inferred using the MS as a feature input to the NN.

In this method, it is important to design the range of the frequency variation. It is determined by the maximum frequency  $f_{\max}$  and minimum frequency  $f_{\min}$  that are allowed to change. In general,  $f_{\max}$  is determined by the sampling time [ms] of the force sensor. The sampling time was 1 ms; therefore,  $f_{\max}$  was 500 Hz. However, it is difficult to calculate  $f_{\min}$  in advance, because  $f_{\min}$  is strongly affected by the frequency of the rotation speed of the tool and the hysteresis value of the force sensor. In addition, when the contact force exceeds a certain level, the rotation of the tool becomes nonuniform, and there is no strong relationship between the contact force and the frequency. Therefore, it is better to set  $f_{\min}$  depending on the task. In this study, we designed the experimental machine such that the frequency varies between 100 Hz and 300 Hz with respect to the contact force, leaving a margin to avoid reaching  $f_{\max}$  and  $f_{\min}$ .

The features to be inputted to the NN must have frequency components between 100 Hz and 300 Hz. At the same time, since the deviations due to hysteresis and offset of the force sensor exist at low frequencies, it is necessary to remove the low-frequency components from the feature values. Therefore, out of the calculated 64-dimensional MS, we deleted the features of the bottom five dimensions and the top 14 dimensions. The low-frequency feature removal should be designed depending on the task. The deletion of the 14-dimensional features above is to remove the effect of noise and to reduce the computational cost. Since the 6th order corresponds to 40 Hz and the 50th order corresponds to 400 Hz, the features are inputted considering only the information from 40 Hz to 400 Hz.

In the field of speech recognition, STFT, MS, and Mel-frequency cepstral coefficient (MFCC) [22], [23] are often used as features. The difference between the STFT and MS is the presence of the Mel frequency transformation, and the difference between MS and MFCC is the presence of a discrete cosine transform. In literature [24], determining the MFCC, which also includes the Mel frequency transform, is considered a promising method for force feature identification; thus, the performances of the three values, namely the STFT, the log transform of STFT (MS), and MFCC, were compared. The results show that the effect of the STFT conversion to the frequency is the most dominant, whereas the conversion to the Mel frequency has a slight effect. However, these results vary depending on the task. We also conducted accuracy verification using each feature to verify the influence of the frequency analysis method.

#### D. Prediction Network based on 1D-CNN

Table I presents the time delay NN (TDNN) model. The TDNN is equivalent to a one-dimensional convolutional NN (1D-CNN) with chronologically ordered information and comprises two convolutional layers and three fully connected layers. ReLU was used as the activation function in both the

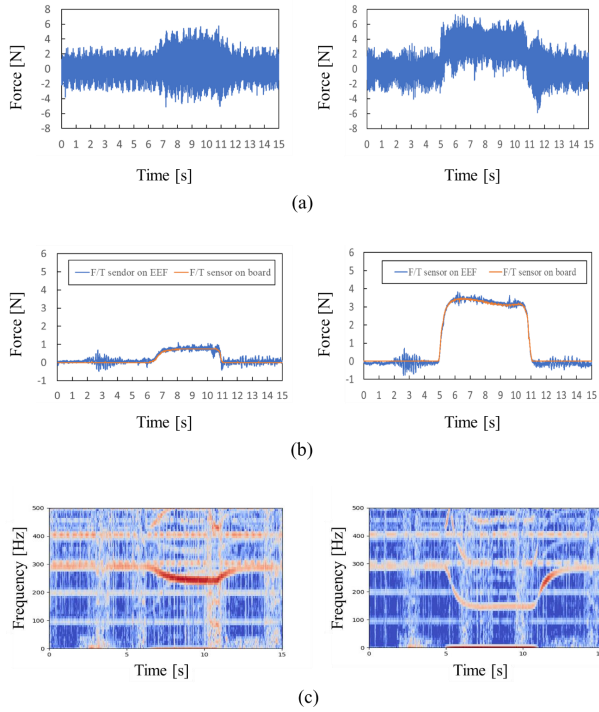


Fig. 6. (a) The force raw data from the EEF force sensor. (b) The force responses of the EEF and worktable-type force sensor. (c) The Mel spectrogram calculated from the force raw data in (a). Dark blue corresponds to low amplitude. Bright red corresponds to high amplitude.

TABLE I  
TDNN BASED ON 1D-CNN

Layer	Filter size	Stride	Output size
Input	-	-	(17, 45)
Conv. 1D	3	1	(15, 20)
Average Pool	2	2	(7, 20)
Conv. 1D	2	1	(6, 10)
Average Pool	2	2	(3, 10)
Fc	-	-	30
Fc	-	-	30
Fc	-	-	1

layers. Adam was used to update the parameters, and the initial learning rate was set to 0.001.

### III. EXPERIMENT

#### A. Control Architecture

A general impedance control system was used; Fig. 7 shows the block diagram of the control system. A disturbance observer (DOB) [25] was used to ensure the disturbance of the position and force control system. Table II lists the control parameters. Here,  $p^{\text{cmd}}$  was created by combining simple linear trajectories, and  $F^{\text{cmd}}$  was taken as a constant. The proposed method is incorporated into the force control system, and the estimated value  $\tilde{F}_{\text{res}}$  is outputted from the output value  $F_{\text{res}}$  of the F/T sensor.

#### B. Preparation of Datasets

To verify the generalization performance of the model, we obtained datasets for four cases. Table III presents the data

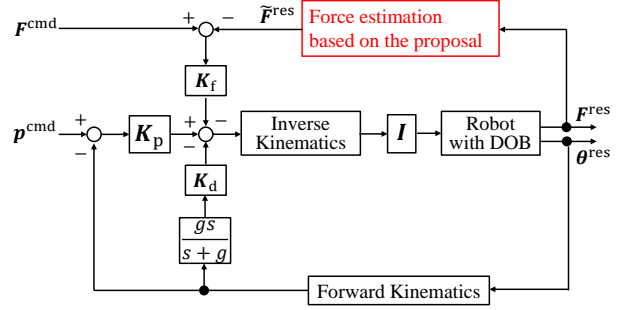


Fig. 7. Block diagram of impedance control based on proposed method.

TABLE II  
PARAMETERS OF CONTROLLER

$K_p$	Proportional gain	diag(700, 700, 150, 1500, 1500, 1500)
$K_d$	Derivative gain	diag(70, 70, 120, 80, 80, 80)
$K_f$	Force gain	diag(0.0, 0.0, 0.1, 0.0, 0.0, 0.0)
$I$	Moment of inertia	diag(1.58, 1.40, 0.80, 0.18, 0.16, 0.04)
$g$	Cutoff freq. of the deriv. filter	10 [Hz]
$T_s^c$	Sample time of the controller	0.001 [s]

acquisition conditions for each dataset. Data1 is a dataset of a simple grinding task without movement of the X-Y plane. In this dataset, as shown in Fig. 6(b), there is no deviation in the force information obtained from the EEF and the worktable-type force sensor, and the contact force is accurately obtained from the force sensor of the EEF. On the other hand, Data2 and Data3 include deviations between the force information obtained from the two sensors, and they are datasets to verify the robustness against deviations (e.g., hysteresis, drift, and offset) in the force information. In this study, we reproduced the deviation in the force information by offset. In Data2, the offset is programmatically shifted by 2 N. In Data3, the offset is shifted by applying a 2 N weight next to the offset acquisition. Data4 is a dataset of linear movement in the X-Y plane after contact, where the origin is the contact point and the translation is 2 cm in the X-axis direction and -3 cm in the Y-axis direction. This dataset is used to verify how the vibration due to the lateral movement and the dynamic friction between the tool and the grinded surface affect the accuracy. Table IV presents the combination of the training and test data. In each case, the training data are set to Data1. In other words, the conditions (b), (c), and (d) in Table IV test how well the model trained on Data1 with simple grinding data can maintain its performance under error-prone conditions.

Because the robot trajectory generation is highly reproducible and the number of data points that can be obtained is not large, the collection of datasets under the same conditions will only yield the relationship between the specific frequency components and the force information. Therefore, we input five patterns of commands in the Z-axis direction of  $p^{\text{cmd}}$ : 0,  $\pm 1$ , and  $\pm 2$  mm. For each command, we obtained 15 and 5

TABLE III  
TYPE OF DATASET

	Offset error	Motion in the X-Y plane
Data1	Not given	None
Data2	Given by programing	None
Data3	Given by weight	None
Data4	Not given	$x = 2\text{cm}, y = -3\text{cm}$

TABLE IV  
TYPE OF DATASET FOR TRAINING AND TEST

	Training	Test	Details to verify effect
a)	Data1	Data1	-
b)	Data1	Data2	Drift of the force sensor
c)	Data1	Data3	Drift of the force sensor
d)	Data1	Data4	Motion of X-Y plane

data points for training and test, respectively. Therefore, each dataset of Data1-4 comprises 75 training data points and 25 test data points. Since we focused on the 1D contact force in this study, only the contact force in the Z-axis direction was obtained.

### C. Performance Evaluation

In this study, we verified the effectiveness of using MS as a feature in the estimation of the oscillatory force information during grinding. For this purpose, we also compared the results with those obtained using the force information.

To reduce the amount of data to be inputted while matching the time-series length, the sampling rate was varied from 1 ms to 2 ms, and the input data were reduced to 256 samples (512 ms).

To compare the prediction accuracy of the model with previous models, we used first-order LPF and feed-forward NN (FNN) as baseline methods in addition to the CNN. The LPF is verified as a widely used method. The FNN has also been used in previous studies [26] for accuracy improvement. In this study, the model is constructed to be optimal for the task and comprises two hidden layers with 50 nodes and an output layer with one node. In the FNN+MS model, the  $45 \times 17$  MS time series data were converted to  $755 \times 1$  1D information as input. ReLU was used as the activation function. In each model, the mean squared error (MSE) was used as the loss function. The learning time was set to 1000 epochs for each model.

Table V compares the root MSEs (RMSEs) of the inference results for each model. From a), the NN is found to be more effective in removing periodic vibration noise with a higher performance than the LPF, and the CNN is suitable for the model. Comparing the results of NN+MS with those of the NN alone in a), it can be confirmed that the estimation accuracy of the NN alone is higher. This result indicates that the performance slightly degraded because the low-frequency component that directly corresponded to the absolute value of the external force was not used. Note that the low-frequency information was removed in the MS, which used only the information from 40 Hz to 400 Hz. The results in b) and c) show that the FNN and CNN were slightly superior to the

LPF and that adding MS as preprocessing significantly improved the performance. These results suggest that a frequency analysis of the force information is effective in the event of drift, because the use of low-frequency response degrades the accuracy in environments that are prone to drift. From the results in d), it can be confirmed that the performance of the proposed method degraded during horizontal movement. Because the state of contact changes during the movement, the relationship between the frequency and the force fluctuates, which affects the force estimation.

The effect on the estimated value is determined by the drift value of the sensor and the noise due to movement. Although the drift value can be designed, the noise generated during the movement is determined by the material of the grinded surface, the grinding tool, and the movement speed of the robot. Therefore, it is difficult to determine the effect on the estimated value in advance. The proposed method is applicable when the position command and other parameters are adjusted so that the drift of the sensor is greater than the effect of noise due to lateral motion.

Table VI shows the RMSE [N] when the low-frequency dimension is removed. Here, “None” represents that the low-frequency dimension is not deleted, and “1-5 dim.” represents that the lower 1-5 dimensions are deleted. Table VI shows that deleting the first dimension makes it more robust against hysteresis in these tasks. The dimension of the hysteresis that is affected depends on the task. Therefore, the number of dimensions of the low frequency to be removed should be designed depending on the task.

To compare the frequency analysis methods, an evaluation test for the force estimation performance was conducted. Fig. 8 shows the results are. Here, all the results except of the CNN only are for the combination with CNN. MS(all) represents the case where all the information up to the 50th order is used, and MS(LC) represents the case where the components up to the 5th order are removed.

A high force estimation accuracy was obtained using only the CNN estimation, and when the frequency analysis was added, the performance was largely the same in all cases. However, when a drift of 2 N occurred, the drift significantly increased the force estimation error. When the STFT, which is one of the simplest frequency analysis methods, was added to the CNN, its error was reduced, and similar results were obtained for the MFCC and MS. These methods reduced the error because the frequency analysis method quantified the change in the frequency depending on the magnitude of the load and sent it to the CNN. However, even when the frequency analysis is implemented, the low-frequency component is affected by drift, and regression methods based on the values affected by drift will generate errors. The fact that the MS(LC) results outperformed the other methods in tests with drift is an indication of the effect of removing components up to the 5th order, which are strongly affected by drift. In addition, this result shows the ability to estimate the external force even with only the high-frequency component, which removes the absolute value of the force. Since the low-frequency component, which is directly related to the external force, is removed in MS(LC), the error is slightly increased

TABLE V  
COMPARISON OF RMSE [N]

	LPF(5Hz)	FNN	CNN	FNN+MS	CNN+MS
a)	0.153	0.107	0.081	0.141	0.147
b)	1.93	1.49	1.48	0.262	0.272
c)	1.91	1.57	1.56	0.285	0.286
d)	0.478	0.376	0.369	0.712	0.655

TABLE VI  
RMSE [N] WHEN LOW-FREQUENCY FEATURES ARE REMOVED.

	None	1 dim.	2 dim.	3 dim.	4 dim.	5 dim.
a)	0.074	0.143	0.170	0.165	0.151	0.147
c)	1.94	0.292	0.275	0.287	0.289	0.286

compared with those of the other methods when there is no drift; nevertheless, it is small compared to the effect of drift.

#### D. Verification of grinding performance

To verify the effectiveness of our proposal, we gave the robot a command to write the letter “A” by grinding. The proposed method is applied as a type of filter to the output value of the force sensor. We also conducted experiments under the condition that there is a deviation in the initial offset to verify the robustness against drift. The results, shown in Fig. 9, indicate that the quality of the grinding work degrades when an offset error occurs in the conventional method, whereas it is only slightly degraded in the case of the proposed method. This result confirms that the proposed method enables robust force control against drift.

#### IV. CONCLUSIONS

In operations with constant vibration, such as grinding and cutting, the vibration frequency has a strong correlation with the external force. Focusing on this characteristic, we proposed an external force estimation method based on the frequency analysis of the force information obtained from a force sensor. The frequency information is found to be more effective for accurate force estimation than the amplitude in operation with large noise caused by vibration. Moreover, it is experimentally demonstrated that the proposed method is more robust against force sensor-specific problems such as hysteresis.

The proposed method is limited to tasks that have a source of vibration at the hand or the contact object, such as grinding or cutting. Since the natural vibration depends on the load of the contact, and its value is always influenced by the force at the hand, in principle, it can be implemented without a large source of vibration. Future work will be to extend this method to more robots by realizing an algorithm that can accurately estimate the external force from minute vibrations.

#### REFERENCES

- [1] D. D. Walker, A. T. H. Beaucamp, D. Brooks, R. Freeman, A. King, and G. Mccavanna: “Novel CNC polishing process for control of form and texture on aspheric surfaces,” in *Proc. Current Development in Lens Design and Optical Engineering III*, vol. 4767, pp. 99–105, 2002.
- [2] Y. Kakinuma, K. Igarashi, S. Katsura, and T. Aoyama: “Development of 5-axis polishing machine capable of simultaneous trajectory posture and force control,” *CIRP Ann.*, vol. 62, no. 1, pp. 379–382, 2013.
- [3] D. Di, J. Polden, J. Dong, and P. Y. Tao: “Sensor guided robot path generation for surface repair tasks on a large scale buoyancy module,” *IEEE/ASME Trans. on Mechatronics*, vol. 23, no. 2, pp. 636–645, 2018.
- [4] X. Xu, D. Zhu, J. Wang, S. Yan, and H. Ding: “Calibration and accuracy analysis of robotic belt grinding system using the ruby probe and criteria sphere,” *Robotics and Computer-Integrated Manufacturing*, vol. 51, pp. 189–201, 2018.
- [5] A. Roswell, F. Xi, and G. Liu: “Modeling and analysis of contact stress for automated polishing,” *International Journal of Machine Tools & Manufacture*, vol. 46, no. 3, pp. 424–435, 2006.
- [6] M. H. Raibert and J. J. Craig: “Hybrid position/force control of manipulators,” *Trans. ASME, J. Dyn. Syst. Meas. Control*, vol. 102, no. 2, pp. 126–133, 1981.
- [7] N. Hogan: “Impedance control Part 1-3,” *Trans. ASME, J. Dyn. Syst. Meas. Control*, vol. 107, no. 1, pp. 1–24, 1985.
- [8] K. Kiguchi, and T. Fukuda: “Position/force control of robot manipulators for geometrically unknown objects using fuzzy neural networks,” *IEEE Trans. on Industrial Electronics*, vol. 47, no. 3, pp. 641–649, 2000.
- [9] C. Schindlbeck, and S. Haddadin: “Unified passivity-based cartesian force/ impedance control for rigid and flexible joint robots via task-

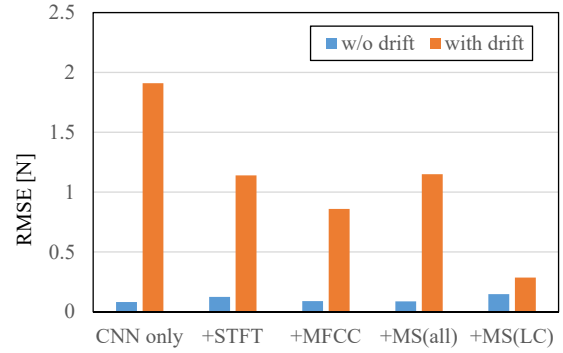


Fig. 8. Comparison of frequency analysis methods.

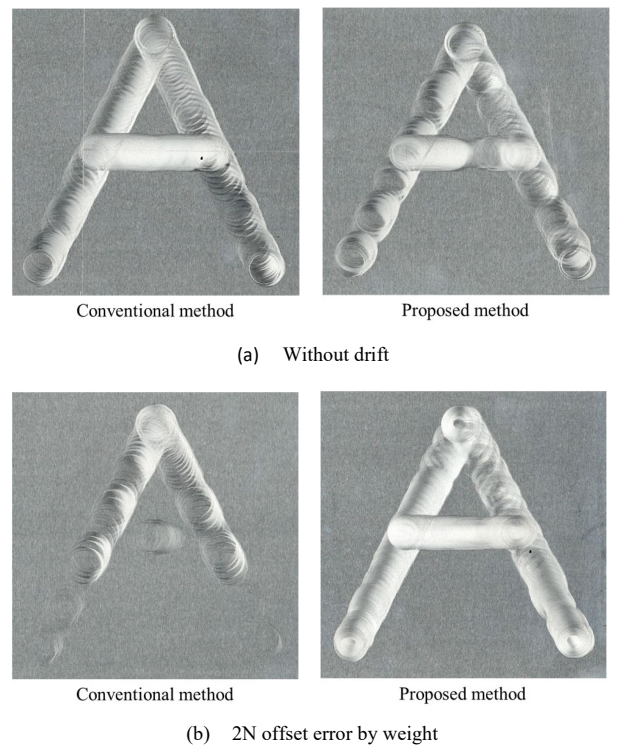


Fig. 9. Results of grinding “A” task.

energy tank,” in *Proc. IEEE International Conference on Robotics and Automation (ICRA)*, pp. 440–447, 2015.

[10] T. Murakami, F. Yu, and K. Ohnishi: “Torque sensorless control in multi-degree -of-freedom manipulator,” *IEEE Trans. on Industrial Electronics*, vol. 40, no. 2, pp. 259–265, 1993.

[11] D. Yunfei, R. Tianyu, K. Hu, D. Wu, and K. Chen: “Contact force detection and control for robotic polishing based on joint torque sensors,” *The International Journal of Advanced Manufacturing Technology*, vol. 107, no. 5–6, pp. 2745–2756, 2020.

[12] J. Pratt, B. Krupp, and C. Morse: “Series elastic actuators for high fidelity force control,” *Industrial Robot: An International Journal*, vol. 29, no. 3, pp. 234–241, 2002.

[13] K. Kong, J. Bae, and M. Tomizuka, “Control of rotary series elastic actuator for ideal force-mode actuation in human–robot interaction applications,” *IEEE/ASME Trans. on Mechatronics*, vol. 14, no. 1, pp. 105–118, 2009.

[14] S. Oh and K. Kong: “High-precision robust force control of a series elastic actuator,” *IEEE/ASME Trans. on Mechatronics*, vol. 22, no. 1, pp. 71–80, 2016.

[15] D. Okumura, S. Sakaino, and T. Tsuji: “High dynamic range sensing by a multistage six-axis force sensor with stopper mechanism,” in *Proc. IEEE International Conference on Robotics and Automation (ICRA)*, IEEE, 2018.

[16] A. Ananthanarayanan, S. Foong and Sangbae Kim: “A compact two DOF magneto-elastomeric force sensor for a running quadruped,” in *Proc. IEEE International Conference on Robotics and Automation (ICRA)*, pp. 1398–1403, 2012.

[17] J. Piao, E. S. Kim, H. Choi, C. B. Moon, E. Choi, J. O. Park, and C. S. Kim: “Indirect force control of a cable-driven parallel robot: Tension estimation using artificial neural network trained by force sensor measurements,” *Sensors*, vol. 19, no. 11, pp. 2520, 2019.

[18] N. Totsu, S. Sakaino, and T. Tsuji: “Development of a desk-type tactile interface using force sensors and an acceleration sensor,” in *Proc. IECON 42nd Annual Conference of the IEEE Industrial Electronics Society*. 2016.

[19] J. Shen, R. Pang, R. J. Weiss, M. Schuster, N. Jaitly, Z. Yang, Z. Chen, Y. Zhang, Y. Wang, R. Skerrv-Ryan, R. A. Saurous, Y. Agiomvrgiannakis, and Y. Wu: “Natural TTS synthesis by conditioning wavenet on MEL spectrogram predictions,” in *Proc. IEEE International Conference on Acoustics, Speech and Signal Processing (ICASSP)*, pp. 4779–4783, 2018.

[20] H. Meng, T. Yan, F. Yuan, and H. Wei: “Speech emotion recognition from 3D log-Mel Spectrograms with deep learning network,” *IEEE Access*, vol. 7, pp. 125868–125881, 2019.

[21] W. Han, C. F. Chan, C. S. Choy, and K. P. Pun: “An efficient MFCC extraction method in speech recognition,” in *Proc. IEEE int. Symp. Circuits Syst.*, pp. 145–148, 2006.

[22] L. Muda, M. Begam, and I. Elamvazuthi: “Voice recognition algorithms using Mel frequency cepstral coefficient (MFCC) and dynamic time warping (DTW) techniques,” *Journal Comput.*, vol. 2, no. 3, pp. 138–143, 2010.

[23] J. Martinez, H. Perez, E. Escamilla, and M. M. Suzuki: “Speaker recognition using Mel frequency Cepstral Coefficients (MFCC) and vector quantization (VQ) techniques,” in *Proc. 22nd International Conference on Electrical Communications and Computers (CONIELECOMP)*, pp. 248–251, 2012.

[24] T. Tsuji, K. Sato, and S. Sakaino: “Contact feature recognition based on MFCC of force signals,” *IEEE Robotics and Automation Letters*, vol. 6, no. 3, pp. 5153–5158, 2021.

[25] K. Ohnishi, M. Shibata, and T. Murakami: “Motion control for advanced mechatronics,” *IEEE/ASME Trans. Mechatronics*, vol. 1, no. 1, pp. 56–67, 1996.

[26] Kim. Y. B., Seok. D. Y., Lee. S. Y., Kim. J., Kang. G., Kim. U., and Choi. H. R: “6-axis Force/Torque sensor with a novel autonomous weight compensating capability for robotic applications,” *IEEE Robotics and Automation Letters*, vol. 5, no. 4, pp. 6686–6693, 2020.